Loss of 5-Hydroxymethylcytosine Is an Epigenetic Hallmark of Melanoma

Christine Guo Lian,[1,2,13] Yufei Xu,[1,13] Craig Ceol,[3,6] Feizhen Wu,[9] Allison Larson,[5] Karen Dresser,[7] Wenqi Xu,[9] Li Tan,[9] Yeguang Hu,[1] Qian Zhan,[2] Chung-wei Lee,[2] Di Hu,[1] Bill Q. Lian,[1,8] Sonja Kleffel,[5] Yijun Yang,[10] James Neiswender,[6] Abraham J. Khorasani,[1] Rui Fang,[1] Cecilia Lezcano,[2] Lyn M. Duncan,[4] Richard A. Scolyer,[11] John F. Thompson,[11] Hojabr Kakavand,[11] Yariv Houvras,[3,12] Leonard I. Zon,[3] Martin C. Mihm Jr.,[5] Ursula B. Kaiser,[1] Tobias Schatton,[5] Bruce A. Woda,[7] George F. Murphy,[2,*] and Yujiang G. Shi[1,9,*]

[1]Division of Endocrinology, Diabetes and Hypertension, Department of Medicine, Brigham and Women's Hospital
[2]Division of Dermatopathology, Department of Pathology, Brigham and Women's Hospital
[3]Stem Cell Program and Hematology/Oncology, Children's Hospital Boston, Howard Hughes Medical Institute, Harvard Stem Cell Institute
[4]Division of Dermatopathology, Department of Pathology, Massachusetts General Hospital
[5]Department of Dermatology, Brigham and Women's Hospital
Harvard Medical School, Boston, MA 02115, USA
[6]Department of Cancer Biology
[7]Department of Pathology
[8]Department of Medicine
University of Massachusetts, Worcester, MA 01605, USA
[9]Laboratory of Epigenetics, Institutes of Biomedical Sciences, Fudan University, Shanghai 200032, P.R. China
[10]ZIOPHARM Oncology, Inc., Charlestown, MA 02129, USA
[11]Royal Prince Alfred Hospital, Melanoma Institute Australia, and Sydney Medical School, The University of Sydney, NSW 2006, Australia
[12]Departments of Surgery and Medicine, Weill Cornell Medical College and New York Presbyterian Hospital, New York, NY 10065, USA
[13]These authors contributed equally to this work
*Correspondence: gmurphy@rics.bwh.harvard.edu (G.F.M.), yujiang_shi@hms.harvard.edu (Y.G.S.)
http://dx.doi.org/10.1016/j.cell.2012.07.033

SUMMARY

DNA methylation at the 5 position of cytosine (5-mC) is a key epigenetic mark that is critical for various biological and pathological processes. 5-mC can be converted to 5-hydroxymethylcytosine (5-hmC) by the ten-eleven translocation (TET) family of DNA hydroxylases. Here, we report that "loss of 5-hmC" is an epigenetic hallmark of melanoma, with diagnostic and prognostic implications. Genome-wide mapping of 5-hmC reveals loss of the 5-hmC landscape in the melanoma epigenome. We show that downregulation of isocitrate dehydrogenase 2 (IDH2) and TET family enzymes is likely one of the mechanisms underlying 5-hmC loss in melanoma. Rebuilding the 5-hmC landscape in melanoma cells by reintroducing active *TET2* or *IDH2* suppresses melanoma growth and increases tumor-free survival in animal models. Thus, our study reveals a critical function of 5-hmC in melanoma development and directly links the IDH and TET activity-dependent epigenetic pathway to 5-hmC-mediated suppression of melanoma progression, suggesting a new strategy for epigenetic cancer therapy.

INTRODUCTION

Melanoma is a unique and highly aggressive type of cancer that occurs more frequently with increasing age and often with a significant contribution of environmental factors to its etiology (Jemal et al., 2001, 2006; Marks, 2000). As one of the most virulent human cancers, melanoma is capable of distant and lethal metastases when the primary tumor volume is as little as 1 mm³. Studies of biomarkers predictive of clinical outcome are impeded by latent periods for detection of metastases that may range from several years to more than a decade, and thus clinically annotated bio-specimen archives serve as valuable surrogates for the otherwise impractical prospective approaches. Such studies are further compounded by the difficulties inherent in the diagnosis of melanoma, as certain benign nevi and melanomas show significant histological overlap. Presently, there is a dearth of molecular markers that facilitate detecting the differences between benign and malignant melanocytic lesions and assist in predicting their biological behaviors. Thus, there is a pressing need for novel biomarkers that define the malignant potential of primary lesions, predict clinical outcome, and forecast therapeutic responses.

Abnormal DNA methylation at the 5 position of cytosine (5-mC) is a well-known epigenetic feature of cancer. Melanoma exhibits global hypomethylation within the bulk genome and local hypermethylation at specific tumor suppressor genes (Hoon et al., 2004; Liu et al., 2008; Shen et al., 2007). Nonetheless, the degree of global hypomethylation in melanoma is not sufficient to distinguish benign nevus from melanoma (Paz et al., 2003). Gene-specific hypermethylation may be a better discriminator, as recent studies indicate that multilocus DNA methylation signature genes may differentiate melanomas from nevi (Conway et al., 2011; Tellez et al., 2009). However, this requires sophisticated molecular biological tools that are not easily applicable

in routine clinical practice, and the small biopsy size of melano-cytic lesions presents another technical limitation. Thus, despite the increasing recognition that abnormal DNA methylation (and/or histone modification) is a crucial participant in melanoma progression, no characteristic epigenetic modifications have been discovered that can be readily used as molecular markers for diagnosis and evaluation of melanoma virulence.

The recent discovery of the ten-eleven translocation (TET) family of 5-mC hydroxylases, including TET1, 2, and 3, which convert 5-mC to 5-hydroxymethylcytosine (5-hmC), also known as the "sixth base," has added an additional layer of complexity to the epigenetic regulation of DNA methylation (Ito et al., 2010; Tahiliani et al., 2009; Zhang et al., 2010). 5-hmC exists at a high level in self-renewing and pluripotent stem cells (Szwagierczak et al., 2010; Tahiliani et al., 2009). However, 5-hmC levels are greatly reduced in most cultured, immortalized tumor cells (Haffner et al., 2011; Song et al., 2011; Yang et al., 2012). Frequent *TET2* mutational inactivation has been reported to associate with decreased 5-hmC levels in various myeloid leukemias (Delhommeau et al., 2009; Langemeijer et al., 2009). In addition, the cofactor α-ketoglutarate (α-KG) is absolutely required and plays a positive and critical role in the conversion of 5-mC to 5-hmC (Xu et al., 2011a). Isocitrate dehydrogenases (IDHs) catalyze oxidative decarboxylation of isocitrate, producing α-KG and CO_2 (Reitman et al., 2011; Xu et al., 2011a). There are two major IDH enzymes in mammalian cells—IDH1 in cytoplasm and its homolog, IDH2, in mitochondria—which catalyze the same reaction. It has been reported that gain-of-function mutations in *IDH1* and *IDH2* in cancer cells produce the oncometabolite 2-hydroxy-glutarate (2-HG), an antagonist of α-KG (Chowdhury et al., 2011; Xu et al., 2011a), which inhibits the TET-mediated conversion of 5-mC to 5-hmC. Moreover, similar to the frequent mutation rate of *IDH1* or *IDH2* in glioma and myeloid leukemia (Dang et al., 2010; Krell et al., 2011), 10% of melanomas harbor a neomorphic mutation in *IDH1* or *IDH2* (Shibata et al., 2011). These studies suggest a role of 5-hmC, TET, and IDH in malignancy. However, it remains elusive as to how 5-hmC is lost and what roles TET and IDH proteins play during tumor progression. In particular, it remains unknown as to how this epigenetic mark and these related enzymes partake in melanoma progression.

Using melanoma as a paradigm of aggressive cancer, here we report that "loss-of-5-hmC" is a new epigenetic hallmark of melanoma. We functionally characterize the significant impact of 5-hmC, IDH2, and TET2 in melanoma progression. Importantly, we show that the activity of IDH2 and TET2 enzymes required for the production of 5-hmC and the re-establishment of the 5-hmC landscape in melanoma cells is essential to regulation of melanoma virulence, contributing to our current understanding of cancer epigenetics.

RESULTS

5-hmC Level Is High in Mature Melanocytes and Nevi and Is Lost in Human Melanomas

High levels of 5-hmC were detected by immunofluorescent (IF) staining in the nuclei of isolated melanocytes that coexpressed MART-1, a melanocyte-specific marker, within the epidermal basal cell layer (Figures 1A and 1B). A more sensitive method

for IF or immunohistochemical (IHC) staining of 5-hmC using HCl-treated formalin-fixed, paraffin-embedded tissue sections resulted in loss of the MART-1 epitope but significantly improved the detection of 5-hmC as demonstrated by staining in normal human tissues (Figure S1A available online). By this method, strong IF staining of 5-hmC was detected in melanocytes within the otherwise negative basal layer, as seen in Figures 1A and 1B, as well as variably within more differentiated suprabasal keratinocytes (Figure 1C). The IF staining pattern was confirmed by IHC staining (Figure 1D), and this more sensitive method for 5-hmC detection was utilized for all subsequent studies of melanocytic nevi and melanomas.

More than 50 individual cases of representative melanocytic lesions, including benign nevi, primary melanomas, and metastatic melanomas, were initially evaluated. Benign nevus cases (n = 30) showed strong nuclear 5-hmC staining, whereas virtually all tumor cells in primary (n = 15) and metastatic (n = 10) melanomas showed partial or complete loss of 5-hmC (Figures 1E–1H). Significant differences in other epimarks were not observed between benign nevi and melanomas (Figure S1B and Table S1), suggesting the unique discriminatory nature of 5-hmC staining as it relates to cells of melanocytic lineage. We next purified genomic DNA from nevi and melanomas and confirmed higher 5-hmC levels in nevi than in melanomas by two independent methods, the anti-5-hmC antibody-based dot blot (Figure 1I) and T4 phage β-glucosyltransferase-mediated 5-hmC glucosylation assay (Figure 1J). Taken together, these data demonstrate that, while a high level of 5-hmC is a distinctive epigenetic signature for melanocytes and benign nevi, significantly diminished or complete loss of 5-hmC is a feature of melanomas.

5-hmC Is a Putative Molecular Marker of Melanoma Progression

We next examined 5-hmC levels by IHC using a melanoma progression tissue microarray (TMA) representing four major diagnostic tumor types: benign melanocytic nevus, primary cutaneous melanoma, melanoma metastases to lymph nodes, and metastases to viscera (Kabbarah et al., 2010; Schatton et al., 2008). Consistent with the individual cases examined above (Figure 1), the TMA confirmed significant 5-hmC loss in primary melanomas and metastatic melanomas compared with nevi (p < 0.001; Figures 2A and S2 and Tables S2 and S3). In two additional commercially available melanoma TMAs, there was significant loss of 5-hmC in melanomas compared to benign nevi (p = 1.1×10^{-7}) and loss in nodal compared to visceral metastases (p = 0.016) (Figure 2B). Taken together, these data further support loss of 5-hmC as a distinctive epigenetic event in melanoma and suggest that 5-hmC may represent a new epigenetic mark for melanoma recognition and progression.

We next correlated the 5-hmC level with critical melanoma staging parameters (tumor depth and mitotic rate) using the melanoma specimens from a clinically annotated cohort including 70 superficial spreading and nodular melanomas (Table S4). There was a negative correlation between 5-hmC staining score and primary melanoma Breslow depth, a standard predictor of prognosis (Figure 2C, r = −0.4, p = 0.0005), as well as between 5-hmC level and mitotic rate (Figure 2D, r = −0.23, p = 0.054). Furthermore, 5-hmC levels were significantly reduced
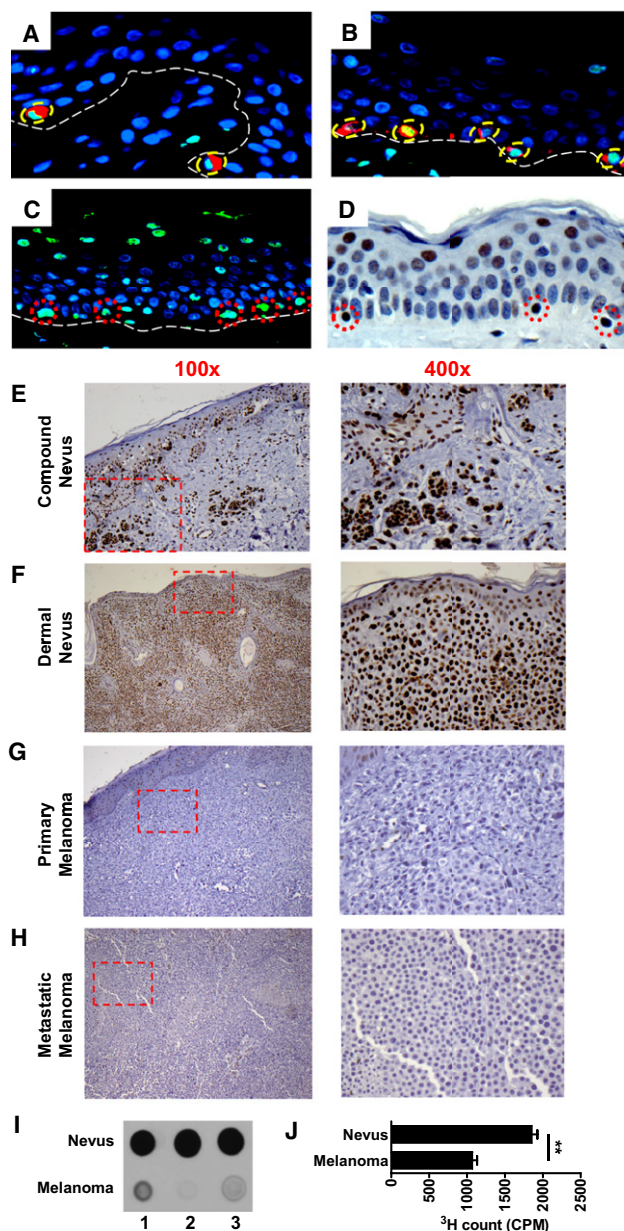
Figure 1. 5-hmC Level Is High in Mature Melanocytes and Lost in Melanomas

(A and B) IF costaining of 5-hmC and MART1 in normal human skin without HCl treatment (400×). Green, 5-hmC; red, MART1; blue, DAPI counterstain of DNA. Among basal-layer cells (dotted white line), 5-hmC-positive cells exclusively proved to be MART-1-positive melanocytes (dotted circles).

(C and D) Detecting 5-hmC in normal human skin by IF (C) and IHC staining (D) with HCl treatment (400×). Both methods showed strong nuclear staining in isolated, solitary cells within the basal layer (dotted circles), in nuclei within the uppermost epidermal layers.

(E–H) Representative histology of 5-hmC IHC staining in the individual cases of benign and malignant melanocytic lesions. Low-power images (100×) on the left column, with the dotted red area magnified at high power (400×) on the right column. All slides were counterstained with hematoxylin (light blue).

(I) Immunoblotting assay shows significantly higher 5-hmC levels in benign nevi than in melanomas. Three representative immunoblot images are shown here from the ten cases of each group.

in melanomas with Breslow values of > 1 mm compared to those with Breslow values of $\leq$ 1 mm (p < 0.01), and melanomas with the presence of > 1 mitosis (a current predictor of nodal metastasis) had less staining than those with $\leq$ 1 mitosis (p < 0.05) (Figure 2E and Tables S5 and S6). Similarly, 5-hmC levels in pathological stage 1 melanomas were significantly higher than in stage 2–3 melanomas (p < 0.05) and were significantly lower in melanoma patients with ulceration (an important staging parameter) than in those without ulceration (p < 0.05) (Figure 2E and Tables S5 and S6). We further analyzed the association between 5-hmC levels and the survival probability based on data for all 70 patients (Table S4). Importantly, Kaplan-Meier curves revealed that patients with 5-hmC-positive melanomas (staining score $\geq$ 1) had significantly higher survival probabilities than patients with 5-hmC-negative melanomas (staining score = 0) at diagnosis (Figure 2F). Thus, loss of 5-hmC in melanoma has both diagnostic and prognostic value in these biospecimen cohorts.

Genome-wide Mapping of 5-hmC in Nevi and Melanomas Reveals a Demolished 5-hmC Landscape in the Epigenome of Melanomas

We next asked whether 5-hmC loss in melanoma is genome wide or loci specific. We first investigated the 5-hmC level changes at specific genomic loci by mapping the genome-wide 5-hmC distribution in nevus and melanoma tissues using a barcoded hydroxymethylated DNA immunoprecipitation (hMeDIP) approach coupled with deep sequencing (hMeDIP-seq) (Xu et al., 2011b) that permits quantitative comparisons of genome-wide changes of 5-hmC between nevi and melanomas (Figure S3A). Similar to our previous finding in mouse ES cells (Xu et al., 2011b), we found that 5-hmC is associated with gene-rich regions in the nevus genome (Figure 3A). Using MACS software (Zhang et al., 2008), we identified a total 54,454 5-hmC peaks in nevi (p < 10^{-5}, FDR < 0.01, fold enrichment > 10) among which more than half are located either in exons (13%) or introns (42.6%), and 13.9% are located at promoters (Figures 3B and S3B). These 5-hmC peaks are associated with 17,468 Refseq genes, in which 15,750 and 10,065 genes are modified by 5-hmC in gene bodies and promoters (−2k to +2k of transcriptional start sites [TSSs]), respectively. There are 8,347 Refseq genes that are modified by 5-hmC both at promoters and in gene bodies. However, we only identified 3,362 5-hmC peaks in melanomas using the MACS software with the same cut-off values as for nevi (Figures 3B and S3B). These peaks are only associated with 3,219 Refseq genes. Importantly, we observed a significantly decreased 5-hmC level within the averaged gene bodies and 20% of their up- and downstream regions in melanomas in comparison to nevi (Figure 3C). Indeed, we identified 41,886 out of 54,454 (77%) total 5-hmC peaks in nevi whose normalized 5-hmC densities were dramatically higher (>5-fold) than in melanomas. These

(J) 5-hmC glucosylation assay confirms that the 5-hmC level in the genomic DNA of nevi is significantly higher than that in melanomas. **p < 0.01 by Student's t test. Data are shown as mean ± SD (n = 3).
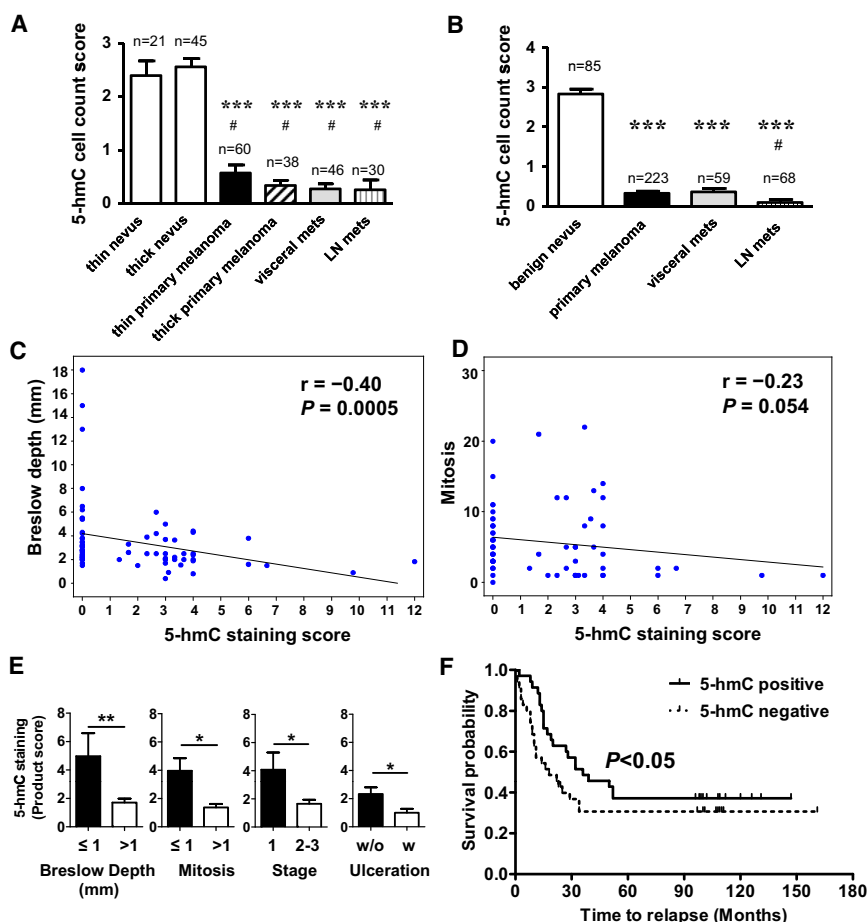See also Figure S1 and Table S1.

Figure 2. Loss of 5-hmC Correlated with Melanoma Progression

(A) Analysis of 5-hmC levels in the SPORE TMA represented by positive cell count score. Each column represents a category of melanocytic lesion (n = number of cases, each case has duplicated tissue cores). Data are shown as mean ± SEM. ***p < 0.001 compared to benign thin nevi; #p < 0.001 compared to benign thick nevi.

(B) Combined cell count scores of 5-hmC staining of three tissue microarrays. Each column represents a category of melanocytic lesion (n = number of cases). Data are shown as mean ± SEM. ***p < 0.001 compared to benign nevus, #p < 0.05 compared to visceral metastases.

(C and D) The Spearman correlation between Breslow depth and 5-hmC staining product score (C) or between mitosis and 5-hmC staining product score (D).

(E) 5-hmC staining product scores are correlated with critical melanoma staging parameters. Data are shown as mean ± SEM. *p < 0.05, **p < 0.01 by Student's t test.

(F) Kaplan-Meier survival curves of melanoma patients with positive 5-hmC staining (solid line) and negative 5-hmC staining (dashed line). p < 0.05 by Gehan-Breslow-Wilcoxon Test.

See also Figure S2 and Tables S2–S6.

41,886 peaks are located in 15,240 Refseq genes at either promoters or gene bodies. Taken together, these analyses indicate that loss of 5-hmC is a genome-wide event during melanoma progression.

We next investigated whether the 5-mC genome-wide distribution is also altered in melanomas. We identified 33,374 and 28,830 5-mC peaks in nevi and melanomas ($p < 10^{-5}$, FDR < 0.01 and fold enrichment > 5), respectively (Figures 3B and S3B). In contrast to 5-hmC, the genome-wide enrichment and distribution pattern of 5-mC is similar between nevi and melanomas, although a slight decrease of 5-mC in melanomas was observed (Figures 3B and 3D), which is consistent with the previously reported global DNA hypomethylation in melanomas (Tellez et al., 2009).

To determine whether gene-specific changes of 5-hmC and 5-mC are associated with melanoma progression, we normalized 5-hmC and 5-mC tag densities in nevus and melanoma samples according to each input sequencing read, which permitted quantitative comparison of 5-hmC and 5-mC signal changes at specific genome loci. Because 5-hmC is converted from 5-mC by TET enzymes, we reasoned that the decreased 5-hmC generation in melanomas would result in the accumulation of its substrate, 5-mC, at certain genomic regions compared to nevi. Indeed, we identified 2,144 peaks at which 5-hmC is dramatically higher (>5-fold) and 5-mC is significantly lower (>2-fold) in 3,401 Refseq gene bodies in nevi compared to melanomas (Figure 3E). Importantly, KEGG pathway enrichment analysis for the 3,401 genes revealed that these genes are closely associated with various melanoma-related pathways, such as adherens junction ($p = 6.05 \times 10^{-9}$), Wnt signaling ($p = 1.67 \times 10^{-7}$), pathways in cancer ($p = 8.65 \times 10^{-7}$), and melanogenesis pathways ($p = 4.84 \times 10^{-4}$) (Figure 3E). As exemplified in Figure 3F, RAC3, IGF1R, and TIMP2 genes show decreased 5-hmC and increased 5-mC in gene bodies in melanomas compared with nevi, and the 5-hmC changes are further verified by conventional hMeDIP-qPCR assays (Figure 3G). Similarly, we also identified 517 peaks at which 5-hmC is dramatically higher (>5-fold) and 5-mC is significantly lower (>2-fold) in 926 gene promoters in nevi compared to melanomas (Figure S3C). Gene ontology (GO) term and KEGG pathway analyses for the 926 genes also show that they are involved in the regulation of cell morphogenesis ($p = 1.18 \times 10^{-4}$), cytoskeleton organization ($p = 0.001$), Ras protein signal transduction ($p = 0.00358$), posttranscriptional regulation of gene expression ($p = 0.0036$) (Figure S3C), and Wnt signaling pathway ($p = 0.009$). The 5-mC and 5-hmC densities at representative gene promoters are shown in Figure S3D.

Thus, this study establishes the genome-wide map of methylome and hydroxylmethylome in nevus and melanoma and reveals the progressive loss of 5-hmC landscape in the epigenome from begin nevus to malignant melanoma. Thus, the demolished 5-hmC landscape is an epigenetic hallmark for melanoma.

Downregulation of *IDH2* and *TET* Family Members in Melanomas

We next sought to determine the imminent cellular factors that are directly responsible for loss of 5-hmC in melanomas. Though the TET family of 5-mC DNA hydroxylases are directly responsible for the generation of 5-hmC (Figure 4A), the catalytic reaction requires cofactor α-KG (Ito et al., 2010; Tahiliani et al., 2009), which is mainly controlled by IDHs (Xu et al., 2011a). Therefore, we hypothesized that IDH and/or TET family enzymes play a critical role in the establishment and maintenance of the 5-hmC landscape in the epigenome of melanocytes and their neoplasms and downregulation of these key enzymes may be responsible for the loss of 5-hmC in melanomas. To test this hypothesis, we first examined the expression levels of *TET* and *IDH* family genes in both nevi and melanomas by RT-qPCR. Whereas *IDH1* has a similar expression level between nevi and melanomas, we found that *IDH2* is significantly downregulated in melanomas (Figure 4B). Strikingly, expression of all three *TET* genes was significantly lower in melanomas than in nevi, with the most dramatic decrease in the *TET2* (Figure 4B). As positive controls, decreased expression of tumor suppressor gene *PTEN* and increased expression of cathepsin B (*CTSB*) gene was observed in melanomas compared to nevi, whereas the expression of housekeeping gene *GAPDH* was unchanged (Haqq et al., 2005; Riker et al., 2008; Talantov et al., 2005). Thus, the dramatically decreased expression of *IDH2*, *TET1*, *TET2*, and *TET3* is specific and may reflect the downregulated nature of these genes in melanomas. Furthermore, the decreased expression of *TET2* in melanomas was confirmed via melanoma cDNA arrays (Figure 4C), and the significantly decreased expression of *IDH2* at the mRNA level was corroborated at the protein level by IHC staining (Figure 4D). These data suggest that the diminished expression of *IDH2* and/or *TET* family genes in melanomas may represent one of the molecular mechanisms underlying global loss of 5-hmC.

Overexpression of *IDH2* in a Zebrafish Melanoma Model Increases 5-hmC Levels and Prolongs Tumor-Free Survival

To test the hypothesis that overexpression of *IDH2* may result in increased 5-hmC levels in melanoma and suppress tumor growth, we employed a recently developed transgenic (Tg) zebrafish model for melanoma, in which BRAF[V600E] is expressed under the control of the *mitfa* gene melanocyte-specific promoter on a p53 mutant background ($p53^{-/-}$) (Ceol et al., 2011). Whereas the 5-hmC level was high in normal zebrafish melanocytes shown by costaining with melanocyte-specific mitfa (Figure 4E), 5-hmC was barely detectable in melanomas of EGFP control animals (Figure 4F, top). *IDH2* overexpression greatly increases the 5-hmC level in melanomas compared to those in EGFP control animals (Figure 4F, bottom), whereas overexpression of catalytically inactive *IDH2 R172K* mutant has not shown any significant effects on the 5-hmC level (data not shown). Strikingly, tumor incidence curve analysis revealed that *IDH2 wild-type (WT)*-overexpressing group, but not *IDH2 R172K*-overexpressing group, showed significantly increased tumor-free survival compared to the EGFP control group (p = 7.8×10^{-9} by log-rank test) (Figures 4G and S4). Collectively,

these data suggest that the isocitrate dehydrogenase activity of IDH2 plays an important role in maintaining proper levels of 5-hmC in melanocytes and may function as a putative tumor suppressor for melanoma progression.

Re-Establishing the 5-hmC Landscape in the Epigenome of Human Melanoma Cells by Reintroducing *TET2*

We next asked whether reintroducing *TET2*, the most dramatically decreased TET family gene in human melanomas, can rescue the demolished 5-hmC landscape in melanoma cells. To exclude the 5-mC hydroxylase-independent function of TET2, we generated pure monoclonal A2058 stable cell lines overexpressing Flag-tagged full-length WT TET2 or the iron-binding site ($H_{1382}RD_{1384}$) disrupted catalytically inactive mutant (TET2 M) (Figure 5A), as well as the vector only control (Mock). The overexpression of full-length TET2 and TET2 M was verified by western blot and RT-qPCR assays (Figures 5B and S5A). We confirmed the global increase of 5-hmC levels in TET2-overexpressing cells, but not TET2-M-overexpressing cells, compared to Mock cells by dot blot and IF assays (Figures 5C and 5D).

We next generated the genome-wide maps of 5-mC and 5-hmC in Mock, TET2-, and TET2-M-overexpressing melanoma cells by MeDIP-seq and hMeDIP-seq, as described above (Figure S3A). Though only marginal changes in 5-mC levels among Mock, TET2-, and TET2-M-overexpressing melanoma cells were observed (Figures S3A and S5B), TET2-overexpressing melanoma cells showed re-establishment of the 5-hmC landscape in their epigenome (Figure 5E). No significant 5-hmC level differences were found between Mock and TET2 M cells. As exemplified by *CCND1* and *MC1R* genes (Figure 5F), deep sequencing data were confirmed by conventional hMeDIP-qPCR assays (Figure 5G).

Further bioinformatic analyses identified 15,835 peaks in TET2-overexpressing cells whose 5-hmC densities are dramatically higher (>5-fold) than in TET2 M cells. Eighty percent (12,752/15,835) of these peaks overlap with a significant portion (30%, 12,752/41,886) of 5-hmC peaks whose 5-hmC levels are dramatically lower (>5-fold) in melanomas than in nevi (Figure 5H, left), suggesting that the 5-hmC landscape in those genomic regions can be re-established by reintroducing *TET2* in human melanoma cells. These overlapping 5-hmC peaks were further analyzed according to their locations (promoter or gene body) at associated genes. We identified 2,664 Refseq genes whose promoters have consistently higher 5-hmC densities in nevi and TET2-overexpressing cells compared to melanomas and TET2 M cells, respectively (Figure 5H, upper-middle). GO term analysis reveals that these 2,664 genes are mainly associated with intracellular signaling cascade, regulation of gene transcription, cell proliferation, and morphogenesis (Figure 5H, upper-right). Similarly, we identified 7,942 Refseq genes whose gene bodies have consistently higher 5-hmC densities in nevi and TET2-overexpressing cells compared to melanomas and TET2 M cells, respectively (Figure 5H, lower-middle). Importantly, KEGG pathway analysis shows an impressive functional association of these genes with various cancer-related pathways, such as focal adhesion (p = 1.9×10^{-12}), pathways in cancer (p = 4.32×10^{-11}), adherens junction (p = 7.94×10^{-10}),
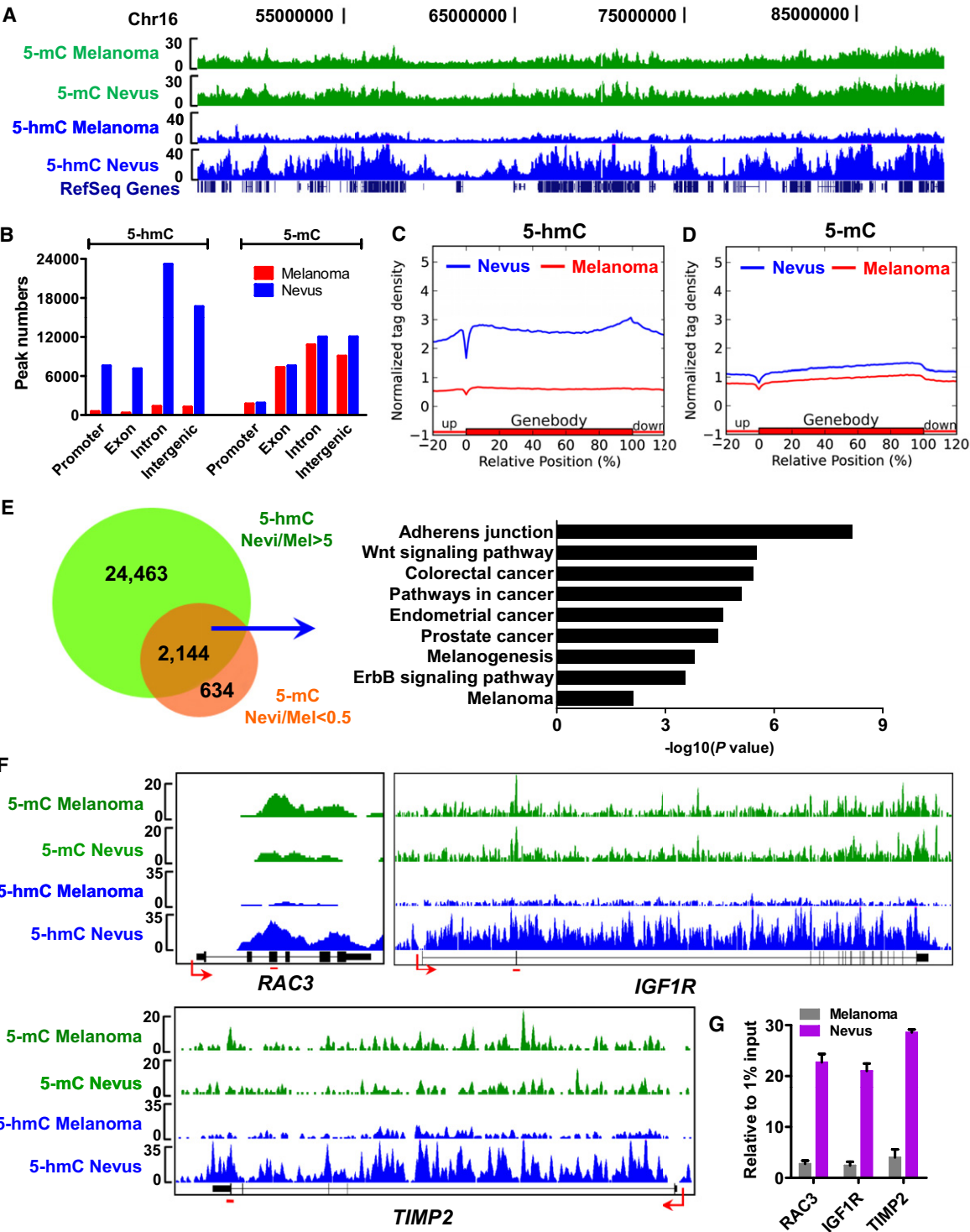
Figure 3. Genome-wide Mapping of 5-mC and 5-hmC in Benign Nevi and Melanomas

(A) The distribution of 5-mC (green) and 5-hmC (blue) densities in the region of chr16:46,651,039-89,749,255 by MeDIP-seq and hMeDIP-seq. Refseq genes are shown at the bottom.

(B) 5-mC and 5-hmC peak numbers of nevus (blue) and melanoma (red) hMeDIP samples in different genomic regions. Promoters were defined as −2k to +2k relative to TSS.

(C and D) Normalized 5-hmC (C) and 5-mC (D) tag density distribution across the gene body. Each gene body was normalized to 0%–100%. Normalized Tag density is plotted from 20% of upstream of TSSs to 20% downstream of TTSs.

and melanoma (p = 5.39 × 10^{-5}) as well as ErbB (p = 3.86 × 10^{-7}) and MAPK (p = 2.29 × 10^{-6}) signaling pathways (Figure 5H, lower-right).

In summary, these biochemical and genome-wide analyses suggest that reintroducing WT TET2, but not the TET2 catalytically inactive mutant, can significantly increase the global 5-hmC level and re-establish, at least in part, the 5-hmC landscape in the epigenome of human melanoma cells, which may subsequently affect several biological processes, such as cancer progression.

Tumor Invasion and Growth Are Suppressed by *TET2*-Mediated Re-Establishment of the 5-hmC Landscape in Melanoma Cells

To determine the biological consequence of *TET2*-mediated re-establishment of the 5-hmC landscape in melanoma cells, we first compared the invasive ability of A2058 cells overexpressing TET2 and TET2 M by in vitro Matrigel assay. Though these two cell lines have similar in vitro proliferation rates (Figure 6A), TET2-overexpressing cells show a significantly lower invasion rate than TET2 M cells (Figure 6B). Next, we investigated the putative tumor suppressor role of 5-hmC and TET2 using in vivo xenograft assays. TET2- and TET2-M- overexpressing melanoma cells were injected into NSG mice, and tumor growth was monitored. TET2-overexpressing melanoma cells gave rise to significantly smaller tumors compared to TET2 M melanoma cells (Figures 6C and 6D). NSG mice injected with Mock melanoma cells showed no significant differences in tumor growth compared to TET2-M-overexpressing melanoma cells (data not shown). Importantly, 5-hmC IHC staining of the xenografted tumor sections showed that smaller tumors derived from TET2-overexpressing cells retained relatively high levels of 5-hmC (Figure 6E, right). Thus, these data highlight a potential tumor suppressor role of increased 5-hmC levels mediated by the enzymatic activity of TET2 in melanoma.

DISCUSSION

Here, we report that loss of 5-hmC is a distinctive epigenetic event of neoplastic progression in melanoma that correlates with clinical relapse-free survival and melanoma staging parameters. Thus, 5-hmC holds promise as a putative molecular biomarker with predictive and prognostic value. The present study also illustrates the genome-wide 5-hmC landscape of benign nevi and melanomas and reveals the strikingly demolished 5-hmC levels and distribution along the epigenome of melanomas in comparison with benign nevi. Furthermore, loss of 5-hmC in melanoma is caused, at least in part, by the decreased expression of key enzymes, IDH2 and TET family proteins, controlling 5-hmC production. In relevant animal models, an increase in 5-hmC levels via either *IDH2* or *TET2*

overexpression is shown to suppress tumor invasion and growth and improve tumor-free survival. Taken together, the present study provides multiple layers of evidence to support that genome-wide loss of 5-hmC is a new epigenetic hallmark of melanoma, with diagnostic and prognostic advantages over global DNA hypomethylation, a recognized epigenetic mark of cancer. Of clinical and therapeutic significance, the present study also opens a new avenue for cancer prevention by targeting the cellular and biochemical pathways that can re-establish 5-hmC levels and landscape in melanoma.

The IHC staining approach to detect 5-hmC may have practical applications clinically. We and others have observed similar loss of 5-hmC in other solid tumors such as breast, ovarian, and colon carcinoma (data not shown) using the same methods (Haffner et al., 2011; Yang et al., 2012). The anti-5-hmC antibody-based IHC strategy could lead to the development of a new, simple, sensitive, and practical adjuvant diagnostic assay. Future studies focusing on borderline lesions and with sufficient clinical outcome annotation are now indicated to evaluate the utility of loss of 5-hmC as a diagnostic and prognostic tool.

The high level of 5-hmC in differentiated and benign nevomelanocytes raises an intriguing question as to the nature of the biological role of 5-hmC in melanocyte differentiation, self-renewal, and malignant transformation. Studies of embryonic stem (ES) cells indicate that 5-hmC may be involved in the regulation of cell differentiation and lineage commitment (Ito et al., 2010; Xu et al., 2011b). Until now, skin-tissue-specific 5-hmC distribution and genome-wide mapping of 5-hmC in cancer have not been well studied. Our findings of a high level of 5-hmC in mature melanocytes and benign nevi, as well as a significantly lower level of 5-hmC associated with melanoma, provide new insights supporting a role of 5-hmC in pathways that are fundamental to cellular differentiation and dedifferentiation. We postulate that the well-controlled dynamic level of 5-hmC during transition from ES cell to melanocyte progenitor to terminally differentiated melanocyte is a epigenetic signature of melanocyte differentiation, the perturbation of which may lead to the induction of oncogenic pathways underlying melanoma progression.

There are several ways to influence 5-hmC levels in cells (Figure 4A). Presumably, dysfunction of TET and/or IDH enzymes, two key factors involved in 5-hmC generation, would greatly reduce 5-hmC generation. Ten percent of melanomas (4/39) harbor an *IDH1* or *IDH2* mutation (Shibata et al., 2011), whereas no *TET* mutations have been reported in melanoma. The low penetration of *IDH* and *TET* mutations in melanoma constitutes robust evidence that other cancer pathways inactivating these 5-hmC-generating enzymes must play a major role in down-regulation of 5-hmC. Herein, we demonstrate the significant decrease in *TET1*, *TET2*, *TET3*, and *IDH2* gene expression in

(E) Peaks at which 5-hmC is significantly reduced (>5-fold) and 5-mC is significantly increased (>2-fold) in gene bodies in melanomas (Mel) compared to nevi (left) and the KEGG pathway analysis results for the associated genes (right).

(F and G) MeDIP-seq and hMeDIP-seq results of *RAC3*, *IGF1R*, and *TIMP2* genes (F) and hMeDIP-qPCR verifications (G). The primer-targeted regions in (G) are noted by red lines in (F). Data are shown as mean ± SD (n = 3) in (G).
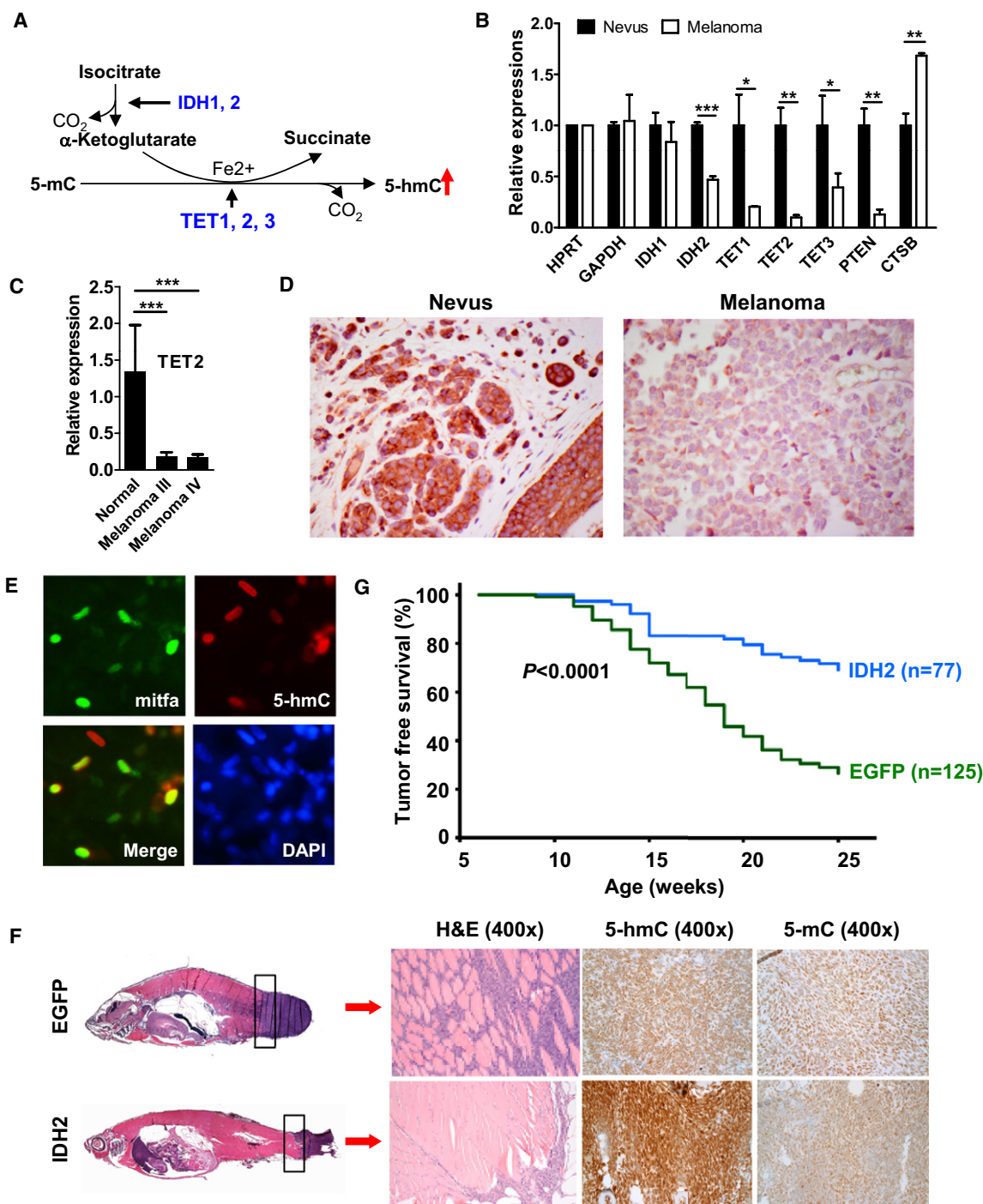
See also Figure S3 and Table S7.

Figure 4. Increased 5-hmC Level by *IDH2* Overexpression in a Zebrafish Melanoma Model Prolongs Tumor-Free Survival

(A) Schematic diagram of 5-hmC generation by the TET family of 5-mC DNA hydroxylases with cofactors α-ketoglutarate and Fe^{2+}.

(B) Relative expression of genes in nevus and melanoma by RT-qPCR. Each gene expression level was normalized to *HPRT* housekeeping gene. Data are shown as the mean of three individual patients ± SEM. *$p < 0.05$, **$p < 0.01$, and ***$p < 0.001$ by Student's t test comparing nevus to melanoma.

(C) Relative *TET2* expression in human melanoma cDNA arrays, including normal skin (n = 3), stage III melanomas (n = 21), and stage IV melanomas (n = 19) by RT-qPCR. Data are shown as mean ± SEM. ***$p < 0.001$ compared the normal skin by Student's t test.

(D) Representative IDH2 IHC staining images in nevi (n = 4) and melanomas (n = 8) at high power (400×).

(E) IF staining of 5-hmC and mitfa in normal zebrafish melanocytes. Green, mitfa; red, 5-hmC; blue, DAPI counterstain of DNA.

(F) Tumors were smaller and less invasive and had higher 5-hmC levels in miniCoopR-*IDH2* zebrafish than miniCoopR-EGFP control zebrafish. Histology of the melanomas from miniCoopR-EGFP control zebrafish and miniCoopR-*IDH2* zebrafish are shown in the left panels. The hematoxylin and eosin staining of tumor

A

Cys-rich Dioxygenase

TET2

$H_{1382}RD_{1384}$

TET2 M

$Y_{1382}RA_{1384}$

B

Mock TET2 M TET2

α-Flag

250kD
150kD
100kD
75kD

α-ACTB

C

TET2 TET2 M Mock

2µg
1µg
5-hmC

2µg
1µg
Methylene blue

D

DAPI Flag 5-hmC Merge

TET2

TET2 M

E

5-hmC

Normalized tag density

— Mock — TET2 — TET2 M

Genebody

up   down

Relative Position (%)

F

5-mC MOCK
5-mC TET2 M
5-mC TET2
5-hmC MOCK
5-hmC TET2 M
5-hmC TET2

CCND1   MC1R

G

hMeDIP

MOCK
TET2 M
TET2

Relative to 1% input

CCND1 MC1R

H

5-hmC peaks Nevus/melanoma>5

29,134
12,752
3,083

5-hmC peaks TET2/TET2 M>5

5,016
2,664
595
Gene promoter

5,722
7,942
587
Gene body

GO term

Intracellular signaling cascade
Negative regulation of gene expression
Negative regulation of transcription
Negative regulation of biosynthetic process
Regulation of MAP kinase activity
Morphogenesis of embryonic epithelium
Protein kinase cascade
TGF beta receptor signaling pathway
Negative regulation of cell proliferation
Regulation of cell morphogenesis

-log10(P value)

KEGG pathway

Focal adhesion
Pathways in cancer
Axon guidance
Adherens junction
Chronic myeloid leukemia
ErbB signaling pathway
Prostate cancer
MAPK signaling pathway
Colorectal cancer
Endometrial cancer
Renal cell carcinoma
Small cell lung cancer
Melanoma
Glioma
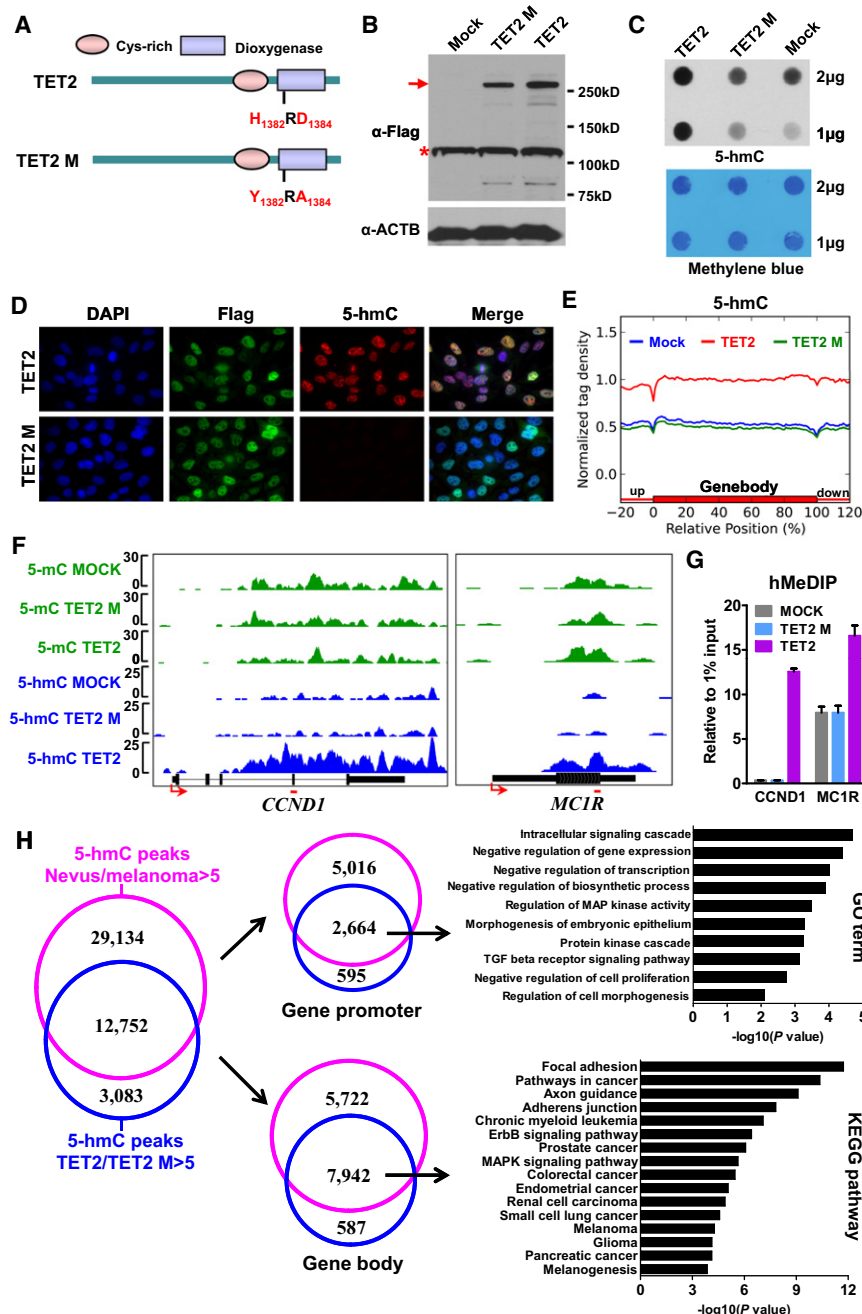Pancreatic cancer
Melanogenesis

-log10(P value)

Figure 5. TET2 Overexpression Re-Establishes the 5-hmC Landscape in the Epigenome of Human Melanoma Cells

(A) Schematic diagram of TET2 WT and TET2 catalytically inactive mutant (TET2 M) proteins.

(B) The expression of Flag-tagged TET2 and Flag-tagged TET2 M proteins by western blot. Red arrow denotes the full-length TET2 and TET2 M bands, and red star denotes nonspecific bands. ACTB was used as a loading control.

(C) Global 5-hmC levels in MOCK, A2058 TET2, and A2058 TET2 M stable cell lines by dot blot assay. The methylene blue staining was used as total genomic DNA loading control.

(D) IF analysis of A2058 TET2 and A2058 TET2 M stable cell lines. The Flag antibody was used to detect Flag-tagged TET2 and Flag-tagged TET2 M. Blue, DAPI counterstain of DNA; green, Flag; red, 5-hmC.

(E) Normalized 5-hmC tag density distribution across the gene body. Each gene body was normalized to 0%–100%. Normalized tag density is plotted from 20% of upstream of TSSs to 20% downstream of TTSs.

(F and G) MeDIP-seq and hMeDIP-seq results of CCND1 and MC1R genes (F) and hMeDIP-qPCR verifications (G). The primer-targeted regions in (G) are noted by red lines in (F). Data are shown as mean ± SD (n = 3) in (G).

(H) Venn diagrams showing the overlap between 5-hmC peaks, which are dramatically higher (>5-fold) in nevi than in melanomas (pink), and 5-hmC peaks, which are dramatically higher (>5-fold) in TET2 overexpression cells compared to TET2 M overexpression cells (blue) (left), and the associated genes according the peak location either at gene promoter (middle-upper panel) or in gene body (middle-lower panel). The GO term and KEGG pathway analyses results are shown in the right panels.

See also Figures S3 and S5 and Table S7.

melanomas compared to benign nevi, which suggests that insufficient enzymes required for the conversion of 5-mC to 5-hmC may account for one of the molecular mechanisms underlying global loss of 5-hmC in melanomas.

In support of this hypothesis, we show that increasing 5-hmC levels and partially re-establishing the 5-hmC landscape in

melanoma cells by restoring expression of active TET2 enzyme, but not the catalytically inactive TET2 mutant, significantly suppresses tumor growth in a murine human melanoma xenograft model. Importantly, this study excludes the possibility that the tumor-suppressive effect is due to the overexpression of

TET2 itself. Rather, such an effect is due to elevated levels of 5-hmC on the genes that are important for key cellular processes. Moreover, we demonstrated that a forced increase in 5-hmC in an established zebrafish melanoma model via overexpression of IDH2 WT, but not IDH2 R172K mutant, significantly suppressed tumor growth and prolonged tumor-free survival.

sections shows an infiltrative pattern of tumor in control miniCoopR-EGFP zebrafish at the body and tail junction, whereas the tumor shows much less infiltrative borders in IDH2-overexpressing zebrafish.

(G) Significant prolongation of tumor-free survival in miniCoopR-IDH2 zebrafish (n = 77) compared with miniCoopR-EGFP control zebrafish (n = 125).
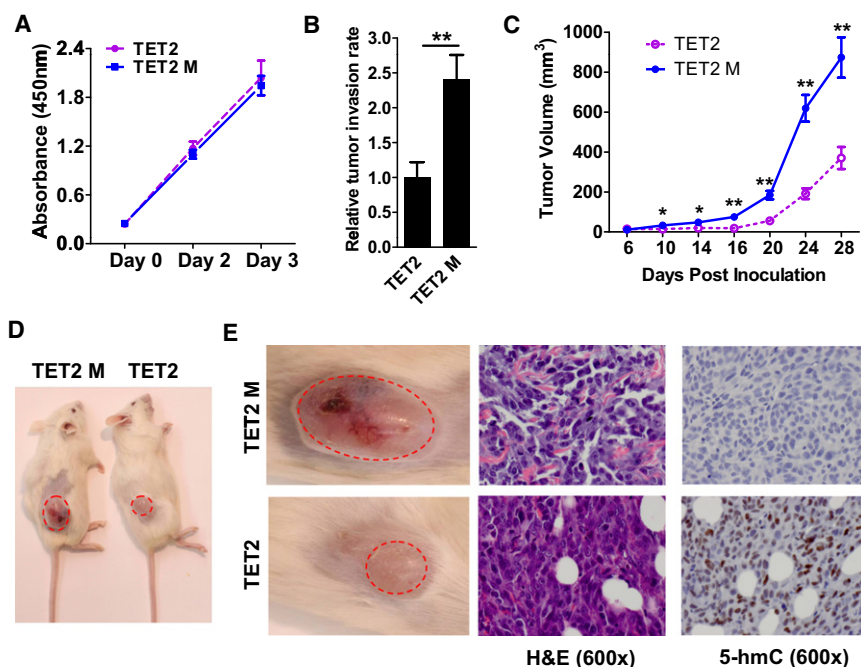
See also Figure S4 and Table S8.

Figure 6. Overexpression of TET2 in Human Melanoma Cells Suppresses Tumor Growth in NSG Xenograft Mice

(A) The proliferation curves of A2058 TET2 and A2058 TET2 M stable cell lines. Data are shown as mean $\pm$ SD (n = 4).

(B) A2058 TET2 melanoma cells show less in vitro invasion than A2058 TET2 M melanoma cells by Matrigel tumor invasion assay. Data are shown as mean $\pm$ SD (n = 3). **$p < 0.01$ by Student's t test.

(C) Tumor growth curves of A2058 TET2 and A2058 TET2 M cells xenografted to NSG mice. Data are shown as mean $\pm$ SEM (n = 10). *$p < 0.05$, **$p < 0.01$ by Student's t test.

(D) Representative images of tumor-bearing NSG mice xenografted with A2058 TET2 M (left) or A2058 TET2 cells (right) at 4 weeks post-inoculation.

(E) H&E and 5-hmC IHC staining of TET2 M (top) and TET2 (bottom) xenografts. The regions shown in left panels are noted by red dash circles in (D).

These data suggest that *IDH2*, but not *IDH1*, is specifically down-regulated in melanomas and that the WT *IDH2* acts as a putative tumor suppressor in the zebrafish melanoma model, although the IDH family of enzymes has been considered candidate oncogenes in various tumors (Ward et al., 2010; Wrzeszczynski et al., 2011). Nonetheless, though the nature of the putative tumor suppressor function of *IDH2* in melanoma and other tumor types warrants future investigations, a dramatic increase in the global 5-hmC level is the most pronounced epigenetic alteration observed in both the *TET2*- and *IDH2*-overexpressing melanoma animal models. Thus, these data demonstrate that high levels of 5-hmC and the appropriate 5-hmC landscape in the epigenome of melanocytes and nevus cells, both potential melanoma progenitors, play a role in preserving the integrity of these indolent cells and in preventing melanoma initiation and progression. Our study supports the novel concept that an elevated level of 5-hmC can serve as a distinctive epigenetic molecular beacon for the reversal of an aggressive melanoma phenotype. It further indicates that particular TET and IDH family enzymes have putative tumor suppressor functions in melanoma progression, and spontaneously targeted down-regulation or inactivation of multiple key enzymes in the 5-hmC-generating pathway is one of the epigenetic mechanisms underlying melanoma development.

The present study also attempts to address the molecular mechanisms directly linking the gene-specific 5-hmC loss to melanoma formation. Genome-wide mapping and comparative analyses of 5-mC and 5-hmC landscape in benign nevi, primary melanomas, MOCK, TET2-, and TET2-M-overexpressing melanoma cells indicated that a program of genes involving various cancer pathways display significant reduction of 5-hmC in comparisons between benign nevi and melanoma, which can be reversed by overexpression of active TET2, but not inactive

TET2 M. However, we did not find simple correlations between significant loss of 5-hmC and expression of associated genes because a reduced 5-hmC level is associated with both up- and downregulated genes in melanomas compared with nevi. This is not surprising because we and others have shown complex roles of 5-hmC in gene transcription regulation in mouse ES cells (Ficz et al., 2011; Xu et al., 2011b). Thus, understanding the intricate relationship between the regulation of 5-hmC and associated gene transcription remains a challenge in 5-hmC biology (Cimmino et al., 2011; Wu and Zhang, 2011). Of note, we identified a subset of genes showing significant 5-hmC level decreases and simultaneous 5-mC level increases in melanomas compared to nevi. The strong association of this subset of genes with various cancer pathways suggests that gene-specific 5-hmC loss may partially contribute to the abnormal DNA methylation pattern in the epigenome of melanoma that has been linked to the progression of various cancers. However, there are a portion of genes showing significant reduction in 5-hmC levels but no obvious 5-mC level changes in melanomas compared to nevi, suggesting that other independent molecular mechanisms, such as 5-hmC-mediated regulation of cell division/replication, cell differentiation/senescence, and/or genome/epigenome instability, may also be involved in linking the loss of 5-hmC to melanoma progression. Future studies aimed at identifying these potential 5-hmC-related mechanisms should enhance insights into 5-hmC function in melanoma formation and progression.

Finally, with melanoma as a paradigm of aggressive cancer, our study provides important insight for future functional studies of 5-hmC in cancer biology. Increasing 5-hmC levels via overexpressing *TET2* reversed the genome-wide 5-hmC distribution from the global 5-hmC loss pattern in melanoma toward a benign nevus-like pattern. More importantly, the phenotype of melanoma was rescued by increasing 5-hmC levels via overexpressing either *TET2* or *IDH2* in animal

models. Thus, loss of 5-hmC in melanoma progression is a fundamental epigenetic event that provides proof of principle that key factors in the 5-hmC-generating pathway can be therapeutically targeted to restore 5-hmC in human melanoma, thus revealing new strategies for the design of melanoma treatment.

EXPERIMENTAL PROCEDURES

Immunohistochemical Staining

Immunohistochemical (IHC) studies employed 5 μm sections of formalin-fixed, paraffin-embedded tissue. Slides were deparaffinized and rehydrated and, after antigen retrieval, were placed in 2N HCl for 30 min, rinsed in distilled water, and placed in 100 mM Tris-HCl (pH 8.5) for 10 min. All were stained on the Dako Autostainer (Dako Corporation, Carpinteria, CA) using the EnVision (Dako) staining reagents. Sections were incubated for 60 min with either rabbit anti-5-hmC at 1:10,000 (Active motif) or mouse anti-5-mC at 1:500 (Eurogentec) and were then incubated with the EnVision+ Dual Link (Dako) detection reagent for 30 min. Sections were washed and treated with a solution of diaminobenzidine and hydrogen peroxide (Dako) for 10 min, and after rinsing, a toning solution (DAB Enhancer, Dako) was used for 2 min to enrich the final color.

Glucosylation of Genomic 5-hmC

Genomic DNA (700ng) purified from benign nevi or melanomas was incubated with 1 μl of T4 phage β-glucosyltransferase (NEB) and 1 μl of UDP-glucose [6-3H] (ARC) in 1 × NEB buffer 4 at 37°C overnight, followed by protease K digestion. DNA was purified, and radioactivity was measured by Beckman Coulter scintillation counter LS6500.

MeDIP-Seq and hMeDIP-Seq

Genomic DNA of human melanomas, nevi, and human melanoma cell lines was purified and sonicated. Illumina barcode adapters were ligated before hMeDIP. Adaptor-ligated DNA (5 μg) was denatured and incubated with 3 μl of 5-hmC antibody (Active Motif) or 10 μg of 5-mC antibody (Eurogentec) at 4°C overnight. Antibody-DNA complexes were captured by protein A/G beads. The immunoprecipitated DNA was purified and sequenced followed by standard Illumina protocols (Xu et al., 2011b). Read sequences were mapped to the human genome (hg19) using ELAND v2 in the CASAVA (Illumina, v1.6) package. Significantly enriched regions were determined by model-based analysis of ChIP-Seq (MACS) package (Zhang et al., 2008). GO term and KEGG pathway analyses were performed by the database for annotation, visualization, and integrated discovery (DAVID) programs (Huang et al., 2009).

NSG Mice Melanoma Xenograft Assay

NOD/SCID interleukin-2 receptor (IL-2R) γ-chain null (NSG) mice were purchased from The Jackson Laboratory (Bar Harbor, ME) and maintained under defined conditions in accordance with institutional guidelines. Experiments were performed according to approved experimental protocols. For tumorigenicity studies, MOCK, WT TET2, or TET2 M A2058 melanoma cells were injected subcutaneously into the flanks of NSG mice (1 × 10^6/injection). Tumor growth was assayed as a time course (Schatton et al., 2008) for the duration of the experiment or until excessive tumor burden or disease state required protocol-stipulated euthanasia.

IDH2 Overexpression in a Zebrafish Melanoma Model

The miniCoopR assay was performed as previously described (Ceol et al., 2011). Transgenes were expressed in zebrafish melanocytes in the background of a stably integrated BRAF^V600E transgene and a p53 loss-of-function mutation. The background also contained a mitfa loss-of-function mutation, which blocked melanocyte development. Transgenes were coupled, via the miniCoopR vector, to a rescuing mitfa gene, ensuring that rescued melanocytes also expressed the transgene being tested. *IDH2* was cloned into the miniCoopR vector, and the resulting miniCoopR-*IDH2* construct was injected into single-cell zebrafish embryos. Transgenic animals were selected

and melanoma onset measured weekly as compared to miniCoopR-EGFP control animals. Animals with melanomas were isolated, and tumors were allowed to progress for 2 weeks prior to being sacrificed. Tumors were formalin fixed, embedded, and sectioned transversely to assess invasion.

ACCESSION NUMBERS

Sequencing data have been deposited to GEO with accession number GSE38231.

SUPPLEMENTAL INFORMATION

Supplemental Information includes Extended Experimental Procedures, five figures, and eight tables and can be found with this article online at http://dx.doi.org/10.1016/j.cell.2012.07.033.

REFERENCES

Ceol, C.J., Houvras, Y., Jane-Valbuena, J., Bilodeau, S., Orlando, D.A., Battisti, V., Fritsch, L., Lin, W.M., Hollmann, T.J., Ferré, F., et al. (2011). The histone methyltransferase SETDB1 is recurrently amplified in melanoma and accelerates its onset. Nature 471, 513–517.

Chowdhury, R., Yeoh, K.K., Tian, Y.M., Hillringhaus, L., Bagg, E.A., Rose, N.R., Leung, I.K., Li, X.S., Woon, E.C., Yang, M., et al. (2011). The oncometabolite 2-hydroxyglutarate inhibits histone lysine demethylases. EMBO Rep. 12, 463–469.

Cimmino, L., Abdel-Wahab, O., Levine, R.L., and Aifantis, I. (2011). TET family proteins and their role in stem cell differentiation and transformation. Cell Stem Cell 9, 193–204.

Conway, K., Edmiston, S.N., Khondker, Z.S., Groben, P.A., Zhou, X., Chu, H., Kuan, P.F., Hao, H., Carson, C., Berwick, M., et al. (2011). DNA-methylation profiling distinguishes malignant melanomas from benign nevi. Pigment Cell Melanoma Res. 24, 352–360.

Dang, L., Jin, S., and Su, S.M. (2010). IDH mutations in glioma and acute myeloid leukemia. Trends Mol. Med. 16, 387–397.

Delhommeau, F., Dupont, S., Della Valle, V., James, C., Trannoy, S., Massé, A., Kosmider, O., Le Couedic, J.P., Robert, F., Alberdi, A., et al. (2009). Mutation in TET2 in myeloid cancers. N. Engl. J. Med. 360, 2289–2301.

Ficz, G., Branco, M.R., Seisenberger, S., Santos, F., Krueger, F., Hore, T.A., Marques, C.J., Andrews, S., and Reik, W. (2011). Dynamic regulation of 5-hydroxymethylcytosine in mouse ES cells and during differentiation. Nature 473, 398–402.

Haffner, M.C., Chaux, A., Meeker, A.K., Esopi, D.M., Gerber, J., Pellakuru, L.G., Toubaji, A., Argani, P., Iacobuzio-Donahue, C., Nelson, W.G., et al. (2011). Global 5-hydroxymethylcytosine content is significantly reduced in tissue stem/progenitor cell compartments and in human cancers. Oncotarget 2, 627–637.

Haqq, C., Nosrati, M., Sudilovsky, D., Crothers, J., Khodabakhsh, D., Pulliam, B.L., Federman, S., Miller, J.R., 3rd, Allen, R.E., Singer, M.I., et al. (2005). The

gene expression signatures of melanoma progression. Proc. Natl. Acad. Sci. USA *102*, 6092–6097.

Hoon, D.S., Spugnardi, M., Kuo, C., Huang, S.K., Morton, D.L., and Taback, B. (2004). Profiling epigenetic inactivation of tumor suppressor genes in tumors and plasma from cutaneous melanoma patients. Oncogene *23*, 4014–4022.

Huang, D.W., Sherman, B.T., and Lempicki, R.A. (2009). Systematic and integrative analysis of large gene lists using DAVID bioinformatics resources. Nat Protocols *4*, 44–57.

Ito, S., D'Alessio, A.C., Taranova, O.V., Hong, K., Sowers, L.C., and Zhang, Y. (2010). Role of Tet proteins in 5mC to 5hmC conversion, ES-cell self-renewal and inner cell mass specification. Nature *466*, 1129–1133.

Jemal, A., Devesa, S.S., Hartge, P., and Tucker, M.A. (2001). Recent trends in cutaneous melanoma incidence among whites in the United States. J. Natl. Cancer Inst. *93*, 678–683.

Jemal, A., Siegel, R., Ward, E., Murray, T., Xu, J., Smigal, C., and Thun, M.J. (2006). Cancer statistics, 2006. CA Cancer J. Clin. *56*, 106–130.

Kabbarah, O., Nogueira, C., Feng, B., Nazarian, R.M., Bosenberg, M., Wu, M., Scott, K.L., Kwong, L.N., Xiao, Y., Cordon-Cardo, C., et al. (2010). Integrative genome comparison of primary and metastatic melanomas. PLoS ONE *5*, e10770.

Krell, D., Assoku, M., Galloway, M., Mulholland, P., Tomlinson, I., and Bardella, C. (2011). Screen for IDH1, IDH2, IDH3, D2HGDH and L2HGDH mutations in glioblastoma. PLoS ONE *6*, e19868.

Langemeijer, S.M., Kuiper, R.P., Berends, M., Knops, R., Aslanyan, M.G., Massop, M., Stevens-Linders, E., van Hoogen, P., van Kessel, A.G., Raymakers, R.A., et al. (2009). Acquired mutations in TET2 are common in myelodysplastic syndromes. Nat. Genet. *41*, 838–842.

Liu, S., Ren, S., Howell, P., Fodstad, O., and Riker, A.I. (2008). Identification of novel epigenetically modified genes in human melanoma via promoter methylation gene profiling. Pigment Cell Melanoma Res. *21*, 545–558.

Marks, R. (2000). Epidemiology of melanoma. Clin. Exp. Dermatol. *25*, 459–463.

Paz, M.F., Fraga, M.F., Avila, S., Guo, M., Pollan, M., Herman, J.G., and Esteller, M. (2003). A systematic profile of DNA methylation in human cancer cell lines. Cancer Res. *63*, 1114–1121.

Reitman, Z.J., Jin, G., Karoly, E.D., Spasojevic, I., Yang, J., Kinzler, K.W., He, Y., Bigner, D.D., Vogelstein, B., and Yan, H. (2011). Profiling the effects of isocitrate dehydrogenase 1 and 2 mutations on the cellular metabolome. Proc. Natl. Acad. Sci. USA *108*, 3270–3275.

Riker, A.I., Enkemann, S.A., Fodstad, O., Liu, S., Ren, S., Morris, C., Xi, Y., Howell, P., Metge, B., Samant, R.S., et al. (2008). The gene expression profiles of primary and metastatic melanoma yields a transition point of tumor progression and metastasis. BMC Med. Genomics *1*, 13.

Schatton, T., Murphy, G.F., Frank, N.Y., Yamaura, K., Waaga-Gasser, A.M., Gasser, M., Zhan, Q., Jordan, S., Duncan, L.M., Weishaupt, C., et al. (2008). Identification of cells initiating human melanomas. Nature *451*, 345–349.

Shen, L., Kondo, Y., Guo, Y., Zhang, J., Zhang, L., Ahmed, S., Shu, J., Chen, X., Waterland, R.A., and Issa, J.P. (2007). Genome-wide profiling of DNA methylation reveals a class of normally methylated CpG island promoters. PLoS Genet. *3*, 2023–2036.

Shibata, T., Kokubu, A., Miyamoto, M., Sasajima, Y., and Yamazaki, N. (2011). Mutant IDH1 Confers an in Vivo Growth in a Melanoma Cell Line with BRAF Mutation. Am. J. Pathol. *178*, 1395–1402.

Song, C.X., Szulwach, K.E., Fu, Y., Dai, Q., Yi, C., Li, X., Li, Y., Chen, C.H., Zhang, W., Jian, X., et al. (2011). Selective chemical labeling reveals the genome-wide distribution of 5-hydroxymethylcytosine. Nat. Biotechnol. *29*, 68–72.

Szwagierczak, A., Bultmann, S., Schmidt, C.S., Spada, F., and Leonhardt, H. (2010). Sensitive enzymatic quantification of 5-hydroxymethylcytosine in genomic DNA. Nucleic Acids Res. *38*, e181.

Tahiliani, M., Koh, K.P., Shen, Y., Pastor, W.A., Bandukwala, H., Brudno, Y., Agarwal, S., Iyer, L.M., Liu, D.R., Aravind, L., and Rao, A. (2009). Conversion of 5-methylcytosine to 5-hydroxymethylcytosine in mammalian DNA by MLL partner TET1. Science *324*, 930–935.

Talantov, D., Mazumder, A., Yu, J.X., Briggs, T., Jiang, Y., Backus, J., Atkins, D., and Wang, Y. (2005). Novel genes associated with malignant melanoma but not benign melanocytic lesions. Clin. Cancer Res. *11*, 7234–7242.

Tellez, C.S., Shen, L., Estécio, M.R., Jelinek, J., Gershenwald, J.E., and Issa, J.-P.J. (2009). CpG island methylation profiling in human melanoma cell lines. Melanoma Res. *19*, 146–155.

Ward, P.S., Patel, J., Wise, D.R., Abdel-Wahab, O., Bennett, B.D., Coller, H.A., Cross, J.R., Fantin, V.R., Hedvat, C.V., Perl, A.E., et al. (2010). The common feature of leukemia-associated IDH1 and IDH2 mutations is a neomorphic enzyme activity converting alpha-ketoglutarate to 2-hydroxyglutarate. Cancer Cell *17*, 225–234.

Wrzeszczynski, K.O., Varadan, V., Byrnes, J., Lum, E., Kamalakaran, S., Levine, D.A., Dimitrova, N., Zhang, M.Q., and Lucito, R. (2011). Identification of tumor suppressors and oncogenes from genomic and epigenetic features in ovarian cancer. PLoS ONE *6*, e28503.

Wu, H., and Zhang, Y. (2011). Mechanisms and functions of Tet protein-mediated 5-methylcytosine oxidation. Genes Dev. *25*, 2436–2452.

Xu, W., Yang, H., Liu, Y., Yang, Y., Wang, P., Kim, S.-H., Ito, S., Yang, C., Wang, P., Xiao, M.-T., et al. (2011a). Oncometabolite 2-hydroxyglutarate is a competitive inhibitor of α-ketoglutarate-dependent dioxygenases. Cancer Cell *19*, 17–30.

Xu, Y., Wu, F., Tan, L., Kong, L., Xiong, L., Deng, J., Barbera, A.J., Zheng, L., Zhang, H., Huang, S., et al. (2011b). Genome-wide regulation of 5hmC, 5mC, and gene expression by Tet1 hydroxylase in mouse embryonic stem cells. Mol. Cell *42*, 451–464.

Yang, H., Liu, Y., Bai, F., Zhang, J.Y., Ma, S.H., Liu, J., Xu, Z.D., Zhu, H.G., Ling, Z.Q., Ye, D., et al. (2012). Tumor development is associated with decrease of TET gene expression and 5-methylcytosine hydroxylation. Oncogene. Published online March 5, 2012. http://dx.doi.org/10.1038/onc.2012.67.

Zhang, H., Zhang, X., Clark, E., Mulcahey, M., Huang, S., and Shi, Y.G. (2010). TET1 is a DNA-binding protein that modulates DNA methylation and gene transcription via hydroxylation of 5-methylcytosine. Cell Res. *20*, 1390–1393.

Zhang, Y., Liu, T., Meyer, C.A., Eeckhoute, J., Johnson, D.S., Bernstein, B.E., Nusbaum, C., Myers, R.M., Brown, M., Li, W., and Liu, X.S. (2008). Model-based analysis of ChIP-Seq (MACS). Genome Biol. *9*, R137.